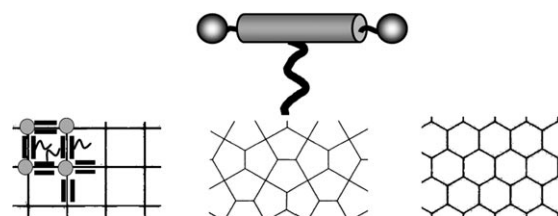


# The Giant-Hexagon Cylinder Network—A Liquid-Crystalline Organization Formed by a T-Shaped Quaternary Amphiphile\*\*

Marko Prehm, Feng Liu, Ute Baumeister, Xiangbing Zeng, Goran Ungar,\* and Carsten Tschierske\*

Supramolecular chemistry is aimed at developing highly complex chemical systems from simple components interacting through noncovalent intermolecular forces.<sup>[1]</sup> A prime objective in this field is to understand and eventually control the transfer of information, imprinted in the molecular tectons, to the supramolecular assemblies.<sup>[2,3]</sup> Liquid-crystalline (LC) phases are relatively simple self-organized structures, formed spontaneously under thermodynamic control, and can therefore be used as model systems for these investigations. Moreover, the combination of order and mobility of these materials is the basis for numerous technical applications, such as, for example, displays, tunable lasers, and phase modulators. Nematic phases, layer-like structures (smectic phases), and regular arrangements of columns (columnar phases) have dominated liquid-crystal research in the past.<sup>[4]</sup>

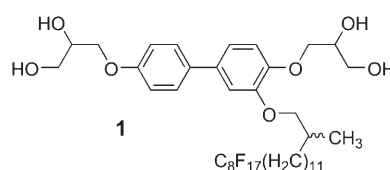
However, recent significant progress in this field has allowed the design of more complex self-organized LC systems. Besides bent-core molecules<sup>[5]</sup> and oligomeric and dendrimeric LC supermolecules,<sup>[6]</sup> complex mesophases have been reported for triblock molecules, composed of a rodlike rigid biphenyl core, two polar hydrogen-bonding groups at the termini, and a nonpolar lateral chain (Figure 1).<sup>[7,8]</sup> These molecules form honeycomb cylinder arrays with a variety of geometries. The nonpolar lateral chains organize into infinite columns, and the rodlike units form shells around them. The polar groups at the ends of the biphenyl cores segregate into



**Figure 1.** Sketch of the molecular structure of bolaamphiphilic block molecules and examples of tiling patterns found for simple cylinder networks of these molecules.<sup>[7b]</sup>

separate hydrogen-bonded columns. The projections of these structures onto the plane normal to the columns can be described as tiling patterns.<sup>[9]</sup> The tiles contain the lateral chains, with the aromatic cores as edges and the hydrogen-bonding sites as nodes. Figure 1 shows three examples of such tilings found in such T-shaped triblock amphiphiles.

Herein we report a new periodic tiling pattern for LC systems, in which the tiles have the shape of a distorted hexagon, with four sides having twice the length of the remaining two. Moreover, the columns inside the honeycomb network have a core-shell structure composed of a fluorocarbon core and a hydrocarbon shell. This new complex LC phase was obtained with compound **1** (Scheme 1), in which a relatively long chain, composed of a branched hydrocarbon spacer segment and a perfluorinated end group, was attached laterally to a biphenyl core that is functionalized at both ends with polar 1,2-diol groups capable of hydrogen bonding.



Cr 60 Col<sub>rec</sub>/c2mm 89 Lam<sub>Sm</sub> 149 Lam<sub>N</sub> 155 Lam<sub>iso</sub> 169 Iso

**Scheme 1.** Structure of **1** with phase-transition temperatures shown (in °C). Phase abbreviations are defined in reference [10].

This compound has a sequence of four different liquid-crystalline phases. The high-temperature phases above 89 °C are lamellar (Lam<sub>iso</sub>, Lam<sub>N</sub>, and Lam<sub>Sm</sub>), identical to those reported earlier for related compounds.<sup>[7b,8]</sup> Here we focus on the low-temperature LC phase occurring below 89 °C. The X-ray diffraction pattern obtained from a surface-aligned sample of this mesophase is shown in Figure 2a,b. It is characterized by a nearly circular diffuse wide-angle scattering halo with a maximum corresponding to the Bragg spacing

[\*] Dr. M. Prehm, Prof. Dr. C. Tschierske  
Institut für Chemie, Organische Chemie  
Martin-Luther-Universität Halle-Wittenberg  
Kurt-Mothes-Strasse 2, 06120 Halle (Germany)  
Fax: (+49) 345-5525-346  
E-mail: Carsten.tschierske@chemie.uni-halle.de

F. Liu, Dr. X. Zeng, Prof. Dr. G. Ungar  
Department of Engineering Materials  
University of Sheffield  
Mappin Street, Sheffield S1 3JD (UK)  
Fax: (+44) 114-222-5943  
E-mail: G.Ungar@sheffield.ac.uk

Dr. U. Baumeister  
Institut für Chemie, Physikalische Chemie  
Martin-Luther-Universität Halle-Wittenberg  
Mühlpforte 1, 06108 Halle (Germany)

[\*\*] The work was supported by the DFG (GRK 894), EPSRC, and ESF (as part of the SONS project SCALES) as well as by the Fonds der Chemischen Industrie and the University of Sheffield (scholarship for F.L.). We thank Dr. C. Martin for help with the synchrotron experiment.

Supporting information for this article is available on the WWW under <http://www.angewandte.org> or from the author.

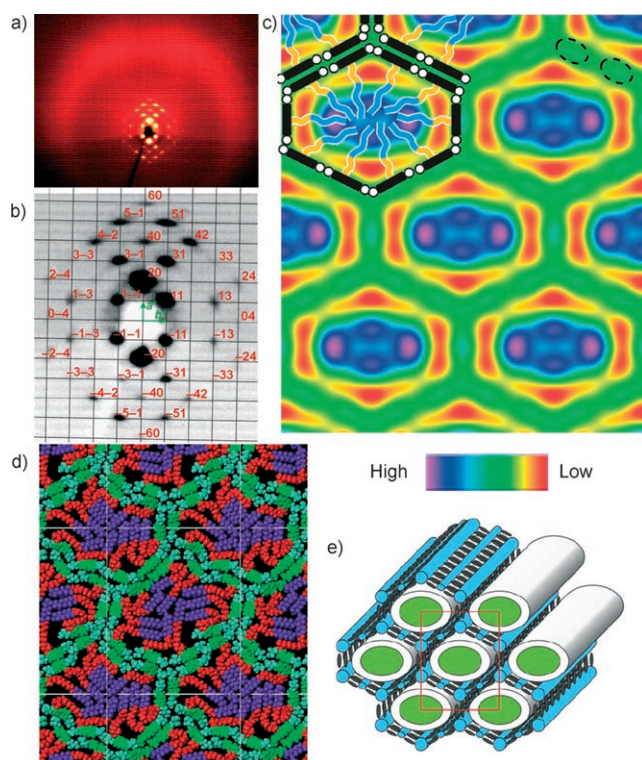


**Figure 2.** The  $\text{Col}_{\text{rec}}/c2mm$  phase of compound **1**: a,b) X-ray diffraction pattern of a surface-aligned sample at 60 °C; the domains are rotationally disordered around the vertical axis perpendicular to the surface and the X-ray beam; c) reconstructed electron-density map obtained from the small-angle diffraction intensities of a powder pattern (color scale at the bottom); dotted ellipses at the right top indicate the position of the aromatic cores in the elongated cylinder sides which have a slightly increased electron density; the organization of the molecules is indicated at the left top; d) snapshot of molecular dynamics simulation; colors: blue/purple = perfluorinated end groups ( $R_f$ ), green = biphenyl, turquoise = diol groups, red = aliphatic chains (for details, see the Supporting Information); e) sketch of the organization of the molecules in the mesophase.

of  $d = 0.52$  nm, which confirms the liquid-crystalline nature of this phase. The sharp small-angle reflections were indexed on a *centered rectangular* lattice, plane group  $c2mm$  with  $a = 8.3$  nm and  $b = 6.7$  nm (at 60 °C). The reconstructed electron-density map (Figure 2c) was obtained from the small-angle diffraction intensities, measured from the high-resolution powder pattern (synchrotron source, see the Supporting Information). In this map the electron density is visualized by spectral colors, where red means lowest electron density and purple identifies regions with highest electron density. The map clearly shows the elliptical cross section of the central high-electron-density region (blue/purple) formed by the fluorinated segments of the lateral chains. This high-density core is surrounded by a shell of lowest electron density (yellow/red) which contains the aliphatic segments of the lateral chains. Each core-shell column is walled off from its neighbors by areas of medium electron density (green) containing the biphenyl cores and diol groups.

These areas have the shape of honeycombs with stretched hexagonal cells in which four sides have approximately twice

the length of the other two. In this medium-electron-density area there are regions with slightly higher electron density (light blue) which are attributed to the biphenyl units. Two of these maxima are located on the longer sides and only one on each of the shorter sides. The electron density is slightly reduced at the nodes and in the middle of the longer sides; these positions are assigned to the hydrogen-bonding networks. The presence of these local maxima can only be explained by an arrangement of the biphenyl units perpendicular to the core-shell columns, and they should be absent for any organization with the biphenyl units parallel to these columns.

The organization of the biphenyl units perpendicular to the core-shell columns is additionally confirmed by the anisotropic swelling and bursting of the polygonal cylinder shells by increasing the temperature, as discussed below. The length of the molecules **1** between the ends of the diol groups is  $L = 1.8$ – $2.1$  nm, depending on the conformation of the terminal diol groups. In the upper left corner of Figure 2c molecules with a length corresponding to 1.8 nm were superimposed onto the electron-density map, which shows that the short walls correspond to a single molecular length, whereas end-to-end pairs of these molecules fit within the length of the extended walls. This result is in line with the interpretation of the local electron-density maxima as positions of the biphenyl cores. The number of molecules in a unit cell, defined by the lattice parameters and a height of 0.45 nm,<sup>[11]</sup> was calculated as approximately 21 on average (see the Supporting Information). As 10 biphenyl cores are arranged in the circumference around each of the core-shell columns, there should be on average two molecules side-by-side in the walls of the polygonal honeycomb. This stipulation is in accordance with the width of these areas (0.9–1.0 nm), corresponding to approximately twice the average diameter of the biphenyl units (0.45 nm each). Figure 2e illustrates schematically the complex structure of this unique LC phase. Accordingly, the biphenyl cores form walls bounding hexagon-shaped channels occupied by the lateral chains. In the circumference of the cylinders 10 molecules are organized so as to form stretched hexagons in which four sides each contain two end-to-end molecules lengthwise, while the remaining two sides comprise the length of only one molecule (hereafter referred to as 2-2-1 hexagons; Figure 3). Figure 2d shows a snapshot of a molecular dynamics simulation of one molecular layer ( $c = 0.45$  nm) after annealing using the experimental  $a \times b$  box with periodic boundaries; the simulation confirms the efficient space filling and phase separation achieved by this structure (see the Supporting Information).

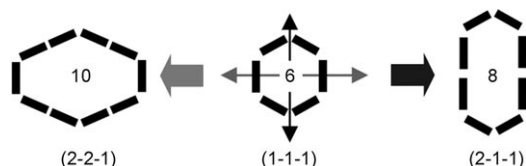


**Figure 3.** Stretching of the regular hexagonal cylinders (1-1-1) of a  $\text{Col}_{\text{hex}}$  phase either along a diagonal or along the normal of two opposite sides gives two distinct cylinder phases with a  $c2mm$  lattice.

This giant-hexagonal cylinder phase is the largest polygonal cylinder phase achieved with this type of molecules, and more generally it represents a new tiling pattern in soft-matter systems. The unique feature is that the hexagons are stretched normal to a side, rather than along a diagonal as in some amphiphiles with nonbranched and shorter side chains (2-1-1 hexagons; Figure 3).<sup>[8b,12]</sup> It would be a challenge to realize this 2-2-1 hexagon motif in other fields of nanoscale engineering, for example, as two-dimensional nets by structural DNA nanotechnology,<sup>[13]</sup> as metal-organic networks,<sup>[14]</sup> or as self-assembled grids on surfaces.<sup>[15]</sup>

When the temperature is increased, the giant-hexagonal cylinders undergo an intriguing process of anisotropic swelling at a constrained perimeter. As shown in Figure 4a, with rising temperature the ratio of lattice parameters  $a/b$  (black circles) increases steeply until it reaches close to 1.358, the

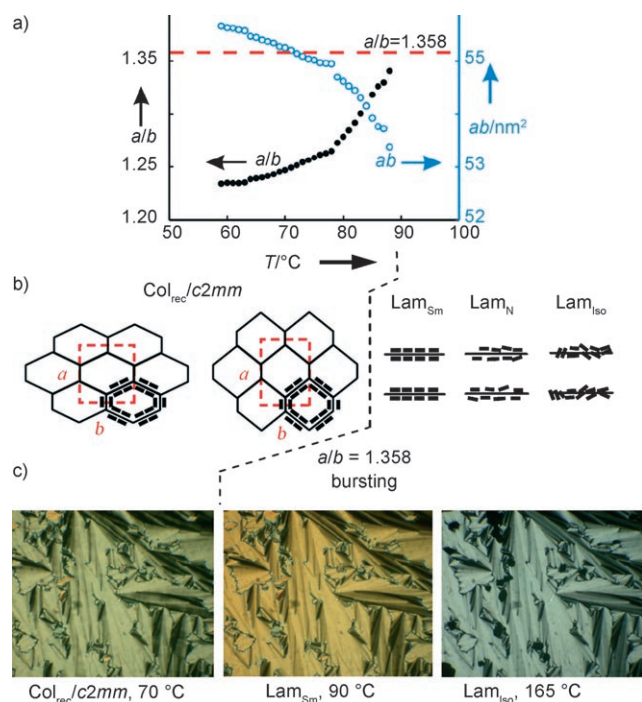


**Figure 4.** Thermotropic transition from the giant-cylinder phase to lamellar phases: a) temperature dependence of the ratio and the product of the lattice parameters; b) models showing the anisotropic swelling (schematic, lateral chains not shown) of the cylinders, followed by bursting and reorganization of the molecules in distinct lamellar phases; c) textures (crossed polarizers).

theoretical value for the maximum area  $ab$  of 2-2-1 hexagons of a given perimeter (see the Supporting Information). Thus, the increased chain coiling at elevated temperatures leads to an expansion of the stretched hexagons along the short axis, compensated by shrinkage along the long axis (Figure 4b). Beyond this limiting  $a/b$  value the volume inside the cylinders would start to decrease again. For this reason an increase in  $a/b$  value beyond 1.358 is impossible, and further increasing the volume of the lateral chains at higher temperature leads to the collapse of the cylinders and the transition to a lamellar structure, as the short sides of the hexagons give way

(Figure 4b). Concomitant with the increase in the  $a/b$  ratio is an overall reduction in the area of the unit cell  $ab$ , and thus a tightening of the column circumference (Figure 4a, blue circles). The latter is assumed to arise from a reduction of the order of the biphenyl cores in the cylinder walls. At elevated temperature there is an increased contribution of biphenyl units tilted away from their preferred orientation perpendicular to the column axis, leading to a reduction of the circumference of the cylinders. The fact that the layer spacing of the lamellar phase ( $d = 4.3$  nm) is approximately half the  $a$  parameter of the centered rectangular phase is in line with the proposed mode of phase transition.

In the two lamellar phases adjacent to the polygonal cylinder phases ( $Lam_{Sm}$  and  $Lam_N$ ) the biphenyl cores remain parallel to the layer planes before the layers become disordered in the  $Lam_{Iso}$  phase (Figure 4b)<sup>[8d,e]</sup> and finally disappear in the isotropic liquid. As the mean direction of the aromatic cores does not fundamentally change during the transition from the  $Col_{rec}/c2mm$  phase to the  $Lam_{Sm}$  phase at 89 °C ( $\Delta H = 0.4$  kJ mol<sup>-1</sup>), there is also no significant change in the texture at this phase transition (Figure 4c); only an increase in the birefringence is seen.<sup>[16]</sup> The birefringence reaches its maximum immediately after the phase transition to the  $Lam_{Sm}$  phase, and upon further heating it decreases again owing to the reduction of the order within the layers on rising temperature ( $Lam_N$ ,  $Lam_{Iso}$  phases; Figure 4c).

In summary, the  $Col_{rec}/c2mm$  phase of compound **1** represents a novel type of complex superstructure obtained by soft-matter self-assembly of appropriately designed low-molecular-weight tectons. It is a new tiling pattern and the first example of a liquid-crystalline core-shell structure embedded in a honeycomb cylinder morphology. In this structure each of the four incompatible molecular moieties is segregated into its own subspace, leading to this unique and complex four-compartment soft-matter structure.

Received: July 16, 2007

Published online: September 4, 2007

**Keywords:** liquid crystals · nanostructures · phase transitions · self-assembly · X-ray diffraction

- [1] J.-M. Lehn, *Proc. Natl. Acad. Sci. USA* **2002**, 99, 4763–4768.
- [2] a) C. Tschierske, *Annu. Rep. Prog. Chem. Sect. C* **2001**, 97, 191–267; b) C. Tschierske, *J. Mater. Chem.* **2001**, 11, 2647–2671; c) T. Kato, *Science* **2002**, 295, 2414–2418; d) I. M. Saez, J. W. Goodby, *J. Mater. Chem.* **2005**, 15, 26–40.
- [3] a) G. Ungar, Y. Liu, X. Zeng, V. Percec, W.-D. Cho, *Science* **2003**, 299, 1208–1211; b) X. Zeng, G. Ungar, Y. Liu, V. Percec, A. E. Dulcey, J. K. Hobbs, *Nature* **2004**, 428, 157–160; c) B. Chen, X.-B. Zeng, U. Baumeister, S. Diele, G. Ungar, C. Tschierske, *Angew. Chem.* **2004**, 116, 4721–4725; *Angew. Chem. Int. Ed.* **2004**, 43, 4621–4625; d) B. Chen, X.-B. Zeng, U. Baumeister, G. Ungar, C. Tschierske, *Science* **2005**, 307, 96–99; e) B. Chen, U. Baumeister, G. Pelzl, M. Kumar Das, X.-B. Zeng, S. Diele, G. Ungar, C. Tschierske, *J. Am. Chem. Soc.* **2005**, 127, 16578–16591.
- [4] D. Demus, J. Goodby, G. W. Gray, H. W. Spiess, V. Vill, *Handbook of Liquid Crystals*, Wiley-VCH, Weinheim, **1998**.
- [5] R. A. Reddy, C. Tschierske, *J. Mater. Chem.* **2006**, 16, 907–961.



- [6] a) V. Percec, G. Johansson, G. Ungar, Y. Zhou, *J. Am. Chem. Soc.* **1996**, *118*, 9855–9866; B.-K. Cho, A. Jain, S. M. Gruner, U. Wiesner, *Science* **2004**, *305*, 1598–1601; b) B. Donnio, D. Guillon, *Adv. Polym. Sci.* **2006**, *201*, 45–155; c) G. Ungar, X. Zeng, *Soft Matter* **2005**, *1*, 95–106.
- [7] a) M. Kölbels, T. Beyersdorff, X. H. Cheng, C. Tschierske, J. Kain, S. Diele, *J. Am. Chem. Soc.* **2001**, *123*, 6809–6818; b) X. H. Cheng, M. Prehm, M. K. Das, J. Kain, U. Baumeister, S. Diele, D. Leine, A. Blume, C. Tschierske, *J. Am. Chem. Soc.* **2003**, *125*, 10977–10996; c) X.-H. Cheng, M. K. Das, U. Baumeister, S. Diele, C. Tschierske, *J. Am. Chem. Soc.* **2004**, *126*, 12930–12940.
- [8] a) M. Prehm, X.-H. Cheng, S. Diele, M. K. Das, C. Tschierske, *J. Am. Chem. Soc.* **2002**, *124*, 12072–12073; b) X.-H. Cheng, M. K. Das, S. Diele, C. Tschierske, *Angew. Chem.* **2002**, *114*, 4203–4207; *Angew. Chem. Int. Ed.* **2002**, *41*, 4031–4035; c) M. Prehm, S. Diele, M. K. Das, C. Tschierske, *J. Am. Chem. Soc.* **2003**, *125*, 614–615; d) N. M. Patel, M. R. Dodge, M.-H. Zhu, R. G. Petschek, C. Rosenblatt, M. Prehm, C. Tschierske, *Phys. Rev. Lett.* **2004**, *92*, 015501; e) N. M. Patel, I. M. Syed, C. Rosenblatt, M. Prehm, C. Tschierske, *Liq. Cryst.* **2005**, *32*, 55–61.
- [9] B. Grünbaum, G. C. Shephard, *Tilings and Patterns*, W. H. Freeman, New York, **1987**.
- [10] Abbreviations: Cr = crystalline solid, Col<sub>rec</sub>/c2mm = rectangular columnar LC phase with c2mm lattice; Lam<sub>sm</sub> = lamellar smectic, Lam<sub>N</sub> = lamellar nematic, Lam<sub>iso</sub> = lamellar isotropic LC phases.<sup>[8]</sup> Iso = isotropic liquid; for analytical data, see the Supporting Information.
- [11] Corresponds to the mean distance between the biphenyl cores, rotationally disordered around their long axis, which form the walls of the polygonal honeycomb.
- [12] The difference between the two distorted hexagonal phases (2-1-1 and 2-2-1) can in some ways be compared to the difference between the “ordered smectic” phases G and H, or I and F. The difference in these smectics is in the direction of molecular tilt, either toward a side or a corner of the hexagonal motif.<sup>[4]</sup>
- [13] C. Lin, Y. Liu, S. Rinker, H. Yan, *ChemPhysChem* **2006**, *7*, 1641–1647.
- [14] a) B. Moulton, M. J. Zaworotko, *Chem. Rev.* **2001**, *101*, 1629–1658; b) K. Takaoka, M. Kawano, M. Tominaga, M. Fujita, *Angew. Chem.* **2005**, *117*, 2189–2192; *Angew. Chem. Int. Ed.* **2005**, *44*, 2151–2154.
- [15] S. Stepanow, N. Lin, D. Payer, U. Schlickum, F. Klappenberger, G. Zoppellaro, M. Ruben, H. Brune, J. V. Barth, K. Kern, *Angew. Chem.* **2007**, *119*, 724–727; *Angew. Chem. Int. Ed.* **2007**, *46*, 710–713.
- [16] At the Col–Lam transition the extended hydrogen-bonding networks are retained, and therefore no significant change can be seen by IR spectroscopy for the position and intensity of the broad  $\nu_{\text{OH}}$  bands.<sup>[7b]</sup>